

Fragmentation of CO_2^{2+} in collisions with low-energy electrons

X. Wang,^{1,2} Y. Zhang,^{1,2} D. Lu,^{1,2} G. C. Lu,^{1,2} B. Wei,^{1,2,*} B. H. Zhang,³ Y. J. Tang,³ R. Hutton,^{1,2} and Y. Zou^{1,2}
¹*Applied Ion Beam Physics Laboratory, Fudan University, Key Laboratory of the Ministry of Education, Shanghai 200433, China*
²*Institute of Modern Physics, Department of Nuclear Science and Technology, Fudan University, Shanghai 200433, China*
³*Research Center of Laser Fusion, China Academy of Engineering Physics, P.O. Box 919-986, Mianyang 621900, China*
 (Received 24 October 2014; published 3 December 2014)

The fragmentation of the CO_2^{2+} dication following 200 eV electron impact double ionization was studied using a cold target recoil-ion momentum spectroscopy. Both two-body and three-body fragmentation channels were observed with an ion-ion coincidence technique. The slopes of the peaks in the coincidence spectra were extracted and compared with previous results and theoretical predictions. Overall, good agreement between theoretical and experimental results was achieved, while different behaviors were observed for the channel of fragmentation into $\text{C}^+ + \text{O}^+ + \text{O}$ with previous high energy electron impact results. The momentum vectors of ionic fragments were measured, and thus the momentum vector of the neutral particle was deduced and kinetic energy release (KER) distributions for the different fragmentation channels were obtained. KER distribution behavior also shows a different signature from that induced by high energy electron impact. Furthermore, the three-body fragmentation mechanism, i.e., dissociation in one- or two-step processes, was distinguished from their distinct signatures on the Dalitz plots and the slopes of the islands from the covariance mapping spectrum. For example, the fragmentation channel $\text{C}^+ + \text{O}^+ + \text{O}$ was found to be very similar to the 60 eV photon impact result [J. Laksman, E. P. Månsson, C. Grunewald, A. Sankari, M. Gisselbrecht, D. Céolin, and S. L. Sorensen, *J. Chem. Phys.* **136**, 104303 (2012)], which shows a predominant sequential dissociation process.

DOI: [10.1103/PhysRevA.90.062705](https://doi.org/10.1103/PhysRevA.90.062705)

PACS number(s): 34.80.Ht, 34.50.Fa, 34.50.Gb

I. INTRODUCTION

Multi-ionization of the diatomic or polyatomic molecule is the subject of numerous studies in recent years [1–7]. Electrons removal from the molecule will result in transitions to excited states of the transient molecular ion, and this, in most cases, will eventually lead to fragmentation. Various projectiles have been applied to generate numerous molecular ions, including synchrotron radiation [6–10], positively and negatively charged ions [2,5,11–16], electrons [4,17–21], and intense lasers [3,22–30].

The early investigations were mainly devoted to cross section, partial cross section studies, and kinetic energy release (KER, defined by the sum energy of all fragments) measurements [8,17,21,22,31]. Recently, with the development of two-dimensional ion-ion coincidence techniques, more and more studies focused on the dynamics and mechanism analysis [3,12,18,32]. In a simplest case where a diatomic molecule dication breaks into two singly charged atomic ions, the ions are then driven purely by the Coulomb force, i.e., the well-known Coulomb explosion; the corresponding kinematics is also simple and intuitive and can usually be well reproduced by the simple Coulomb explosion model. Nevertheless, for the triatomic or polyatomic molecule or when the cluster breaks into three or more fragments, the situation becomes be very complicated. As a simple triatomic molecule, CO_2 has drawn a lot of interest. In this case, the simplest fragmentation mechanism is the synchronous concerted Coulomb explosion, in which all bonds break up simultaneously and the charged fragments are driven purely by Coulomb force. Alternatively, the bonds can break up in a sequential or stepwise manner, e.g., the molecular ions break in two different steps, thus termed as a

two step or sequential process. Moreover, there is a scenario in between these two above, the asynchronous breakup, in which the bonds break in a single step but at a time where the vibration and rotation processes precede the fragmentation. Although numerous studies have been performed to investigate the breakup mechanism for CO_2^{2+} and CO_2^{3+} [1,3,5,6,12] with ions and laser as perturbation, the electron-impact ionization of CO_2 and its subsequent dissociation mechanisms studies under impact energies are scarce in the available literature [4,18–20,33].

In the present work, a cold target recoil ion momentum spectroscopy (COLTRIMS) was adopted to study the fragmentation of CO_2^{2+} formed in low energy electron induced ionization of CO_2 . By measuring the momentum vectors of the fragment ions in coincidence, the KER distributions and the slopes in the two-dimensional ion-ion coincidence map for different dissociation channels were obtained. The results are compared with previous works for different projectiles. With the help of Dalitz plots, we are able to distinguish the concerted or sequential mechanisms of the fragmentation.

II. EXPERIMENTAL SETUP AND DATA ACQUISITION

The experiment has been performed on the COLTRIMS at Fudan University, Shanghai. A detailed description about the setup can be found in [34,35]. Briefly, a thermocathode electron gun provides a pulsed electron beam with energy ranging from a few eV up to 2 keV [36]. The pulse width of the electron beam is determined by a fast pulse voltage power supply (+50 V, 1 ns), which is floated on a grid electrode in front of the electron gun anode with a bias voltage of -25 V with respect to the gun cathode. A pair of coils was used to shield the background magnetic field, making sure that the residual magnetic field is lower than 10% of the earth's magnetic background. The beam current was optimized to

*brwei@fudan.edu.cn

reduce double hit events and preserve a reasonable count rate at the same time, and the repetition rate of the electron pulse was kept at 15 kHz. A multistage pumping system was used to generate the supersonic gas jet: high pressure gas of 2 bar was injected into the first stage of the chamber through a 10 μm nozzle and then selected by two skimmers with sizes of 0.1 and 0.5 mm, respectively. The distance between the nozzle and the first skimmer is variable around 10 mm, and the vacuum at the collision chamber is about 2×10^{-10} torr.

The recoil-ions were extracted perpendicularly to the electron beam. The extraction field (~ 50 V/cm) was switched on a few ns after the collision to eliminate the influence on the incident electron beam. A time-focusing geometry is adopted to reduce the influence of the expansion due to the delayed extraction, i.e., the fragments will first expand for a few nanoseconds and when the extraction field is switched on, the ions were accelerated to about 500 eV in 10 cm, passing through a field free region of 20 cm length, and finally recorded on the time and position sensitive detector, composed of microchannel plates and a delay-line anode. A high performance multihit time to digital Converter (TDC) with a 52 μs full scale range and 5 ns double hit resolution was adopted here and the measurement was recorded event by event. During the experiment, the recoil-ion signals served as starts, and the delayed pulse signal of the electron beam was used as a common stop of a measurement event. Using standard COLTRIMS methodology, three-dimensional momentum vectors of all charged fragments can be reconstructed, and thus KER distributions and an ion-ion coincidence map can be obtained.

III. RESULTS AND DISCUSSION

The ion-ion coincidence spectrum is shown in Fig. 1. Three pronounced fragmentation channels are observed and

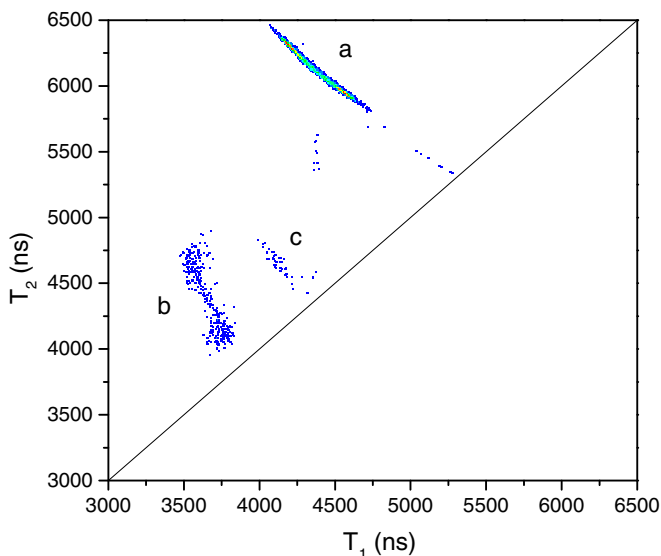
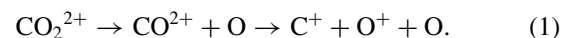


FIG. 1. (Color online) Ion-ion coincidence map obtained in 200 eV electron collision with CO_2 (raw data). Three pronounced channels are from a, $\text{O}^+ + \text{CO}^+$; b, $\text{C}^+ + \text{O}^+ + \text{O}$; and c, $\text{O}^+ + \text{O}^+ + \text{C}$.

termed as *a*, *b*, and *c* respectively. The sharp and narrow island *a* corresponds to the dissociation channel of $\text{O}^+ + \text{CO}^+$. This is in excellent agreement with expectation of the Coulomb explosion picture as it is just a simple two-body separation. However, the islands *b* and *c*, which correspond to the dissociation channels of $\text{C}^+ + \text{O}^+ + \text{O}$ and $\text{O}^+ + \text{O}^+ + \text{C}$, respectively, are much broader due to the release of a neutral atom. According to momentum conservation, the neutral atom's momentum blurred the sharp distribution and changed the slopes of the islands which will be discussed later. In the middle of island *b*, the number of counts is lower; this is because the extraction field is not high enough to collect the highly energetic O^+ and C^+ ions which were emitted perpendicularly with respect to the time of flight (TOF) direction.

These islands are in good agreement with previous studies by Bhatt *et al.* for an electron energy of 12 keV [4]. However there are also some differences. First of all, although C^{2+} peak was observed in the TOF spectrum (not shown in the present work), no coincidence events were found for fragmentation of triply ionized CO_2 in our case, for example, channel $\text{CO}_2^{3+} \rightarrow \text{C}^{2+} + \text{O}^+ + \text{O}$. As mentioned above, we reduced the electron beam intensity to reduce the false coincident rate; thus we attribute the absence of the fragmentation of triply ionized CO_2 to the low cross section at such low incident electron energy. Second, a thin coincidence line at the vicinity of the $\text{O}^+ + \text{CO}^+$ island (*a* of Fig. 1) is presented in our spectrum. This may be attributed to a channel $\text{CO}_2^{2+} + \text{CO}_2^{2+}$ at the first sight just from the TOFs, but it is actually from the decay of metastable CO_2^+ . Although the dimer $(\text{CO}_2)_2^+$ was observed in the TOF spectrum which originated from the supersonic gas jet due to the low temperature of the target, the fragmentation channel of $\text{CO}_2^+ + \text{CO}_2^+$ was not observable on the covariance mapping spectrum; thus we are sure that the thin coincidence line is not the channel $\text{CO}_2^{2+} + \text{CO}_2^{2+}$, but the fragmentation of metastable CO_2^+ as pointed out by Tian and Vidal [18]. As the collinear configuration of CO_2^{2+} has a shallow potential well above the dissociation limit of $\text{O}^+ + \text{CO}^+$, the dissociation may happen after a long lifetime, which has been estimated to be around 900 ns. Therefore, when the fragmentation happens at the drift region, where the velocity is no longer related to the charge to mass ratio, their TOFs will be eventually similar to those of their parent ion CO_2^{2+} ; consequently the thin line is formed around the TOF of CO_2^{2+} .

As suggested by Eland and coauthors [6], the slopes of the islands are related to different reaction mechanisms, especially for three-body breakup processes. For the two-body Coulomb explosion process the slope should simply be $-q_1/q_2$ as a consequence of momentum conservation, where q_1 and q_2 correspond to the charges of the first and second ion, respectively. For three-body fragmentation, things get complicated. For the two step fragmentation of CO_2^{2+} , there are two different types of charge separation. The charge can be separated in the second step, for example:



This is termed as deferred charge separation. The slope in this case is $-(q_1/q_2)$. Otherwise, if the charge is separated in the first step (initial charge separation), again the fragmentation

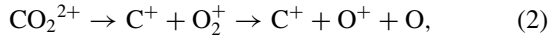
TABLE I. Comparison of the slopes of different channels observed in a two-dimensional coincidence map obtained by 200 eV impact double ionization of CO₂. Two-step (i)₁ and Two-step (i)₂ represent C⁺ released in the first/second step, respectively, of the initial charge separation mechanism. Two-step(d) represents the deferred charge separation.

Fragmentation channel	Theoretical predictions				Electron impact		
	Two-step(i) ₁	Two-step(i) ₂	Two-step(d)	Concerted	Present work	0.6 keV ^a	12 keV ^b
O ⁺ + CO ⁺				−1	−1.01 ± 0.01	−1.00 ± 0.02	−1.00 ± 0.02
C ⁺ + O ⁺ + O	−0.5	−2.33	−1.0	∞	−1.75 ± 0.04	−2.75 ± 0.04	−2.75 ± 0.04
O ⁺ + O ⁺ + C	−0.57		−1.0	−1	−1.03 ± 0.03	−1.00 ± 0.02	−1.00 ± 0.02

^aReference [4].

^bReference [18].

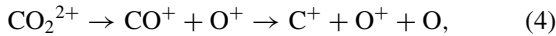
can be categorized into two: if the lighter fragment ion is released in the first step or the second step. For example, in the case



the lighter ion C⁺ is released in the first step, and the slope should be

$$-(q_1/q_2) \frac{m_2}{m_2 + m_3}, \quad (3)$$

where m_1 , m_2 , and m_3 correspond to the mass of the lighter ion, the heavier ion, and the neutral atom, respectively. While in the case



C⁺ is released in the second step, and the slope should then be

$$-(q_1/q_2) \frac{m_1 + m_3}{m_1}. \quad (5)$$

It should be noted that for both synchronous and asynchronous concerted fragmentation processes, because of the linear configuration of the CO₂ molecule, a C⁺ ion is expected to carry much less momentum compared to an O atom and an O⁺ ion. This means that the island on the ion-ion coincidence map should almost be vertical.

Experimental results of the corresponding fragmentation channels' slopes were extracted and fitted with the method of least squares. The comparison between theoretical predictions and experimental results is listed in Table I. In general good agreement is achieved between our results and theoretical predictions.

For O⁺ + CO⁺, all the experimental results are around −1, which is a benchmark of the Coulomb explosion model. For the O⁺ + O⁺ + C channel, again all the experimental result are around −1. As a result of the linear configuration, the deferred charge separation requests isomerization to form O₂²⁺ in the first breakup step, it is very unlikely to occur. Thus the slope of −1 indicates the predominant contribution of the concerted fragmentation.

For the C⁺ + O⁺ + O channel, our result shows a slope of −1.75 ± 0.04, which is quite different from the result of −2.75 ± 0.04 of Ref. [4], where they argued that it originates from a predominant contribution from the initial charge separation of the sequential process [Two-step(i)₂ in Table I] with a mixture of contributions from the concerted mechanism.

Our result also shows the significant contribution from Two-step (i)₂ for this fragmentation channel, but it's not dominant. As Two-step (i)₁ is unlikely to happen because of the low isomerization cross section to form O₂⁺, it seems that the deferred charge separation also plays a certain role in this situation.

Taking advantage of COLTRIMS, the momenta of ionic fragments in all three dimensions were measured and the momentum of the neutral atom can be deduced from momentum conservation. Therefore the KER distributions of different fragmentation channels can be obtained. Compared to the high energy electron impact result, the KER distributions of the three-body fragmentation channels behave quite differently. As shown in Fig. 2, in the present work the KER of the O⁺ + O⁺ + C channel is lower than that of the channel C⁺ + O⁺ + O. This can be easily explained with the Coulomb explosion picture, since the distance between the two oxygen atoms is larger than that between carbon and oxygen due to the linear configuration, the KER of the channel C⁺ + O⁺ + O should be correspondingly large. As mentioned above, this is just the opposite in [4]; in their case of 12 keV electron impact, the KER distribution for the O⁺ + O⁺ + C channel is narrower than that for the C⁺ + O⁺ + O channel. This suggests that at high electron energies, higher electronic states are involved, which might cause the failure of Coulomb explosion picture.

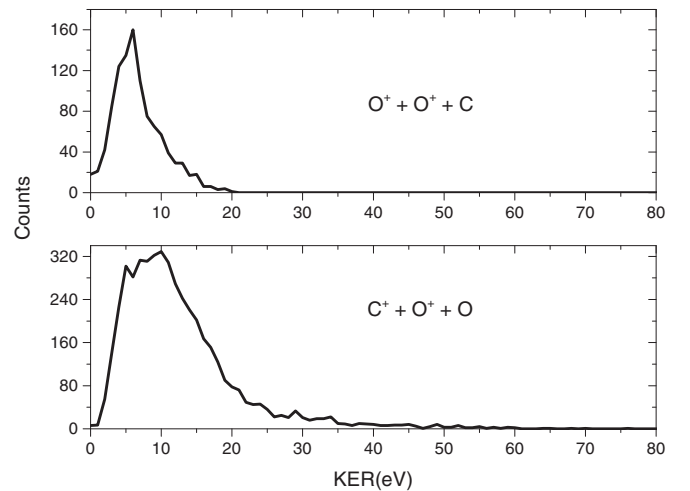


FIG. 2. KER distributions for three-body fragmentation of CO₂²⁺ induced by 200 eV electron impact.

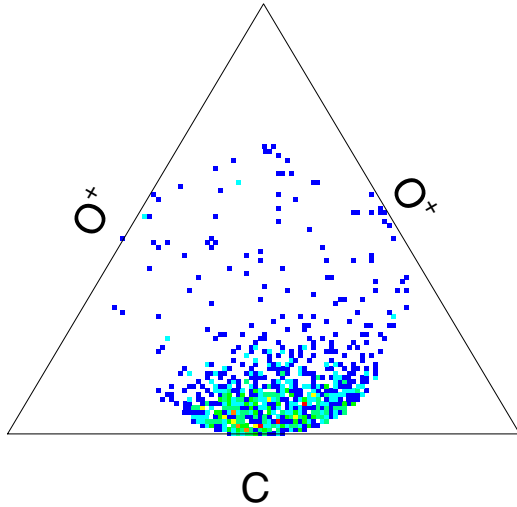


FIG. 3. (Color online) Dalitz plot for the three-body fragmentation of $\text{CO}_2^{2+} \rightarrow \text{O}^+ + \text{O}^+ + \text{C}$ induced by 200 eV electron impact.

To further investigate the fragmentation mechanisms, the momentum balance of the three-body fragmentation process is presented in Dalitz plots (Figs. 3 and 4). Dalitz plots have been widely used [1,12,37,38] in fragmentation mechanism studies. In a Dalitz plot, the data is plotted within an equilateral triangle. Each edge of the triangle represents one of the final-state fragments. The distances between a data point and the three edges are the corresponding relative squared momenta $\pi_i = p_i^2 / \sum p_j^2$, where p_i and p_j are the momentum of the i th and j th particle respectively. As we see in Fig. 3 for the channel $\text{O}^+ + \text{O}^+ + \text{C}$, the dominant data points are close to the C edge; this indicates the dominant momentum is shared by the two O^+ ions. This is consistent with previous analysis for the slope of this fragmentation channel: the dominant concerted fragmentation mechanism results in a strong correlation in the

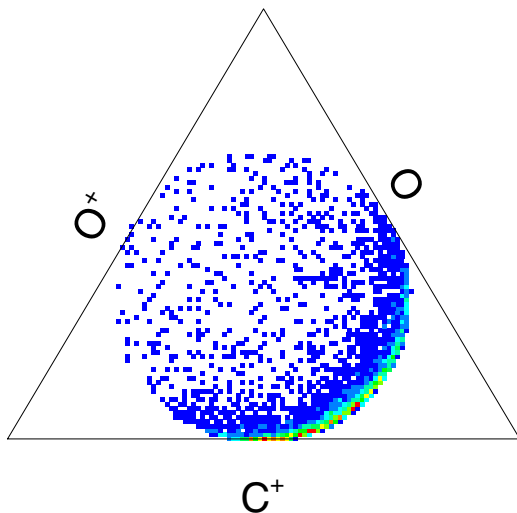


FIG. 4. (Color online) Dalitz plot for the three-body fragmentation of $\text{CO}_2^{2+} \rightarrow \text{C}^+ + \text{O}^+ + \text{O}$ induced by 200 eV electron impact.

two O^+ ions. The small momentum of the C atom agrees with the broad structure on the covariance map.

The Dalitz plot for the channel $\text{C}^+ + \text{O}^+ + \text{O}$ is presented in Fig. 4; it is very similar to the result of the 60 eV photon impact in [1]. The most pronounced structure is the nearly symmetric distribution around the maximum O^+ momentum. This is the typical signature of two-step dissociation [38], in which O^+ is emitted in the first step, leaving the C^+ and O atom anticorrelated. Meanwhile, the data points close to the C^+ and O atom edges of the triangle are more pronounced than in the 60 eV photon impact case. The points close to the O atom edge correspond to the deferred charge separation of the two-step fragmentation. In this case the primary fragment is the neutral O atom with a small momentum; the momentum balance of the C^+ and O^+ released in the second step will result in a slope of -1 . Again, this is in consistency with the previous analysis. The points close to C^+ edge, however, are typically from the concerted fragmentation mechanism [1] due to the linear structure as discussed above. This can not be distinguished just from the slope.

IV. CONCLUSIONS

The fragmentation of the CO_2^{2+} dication by 200 eV electron impact was investigated using a cold target recoil-ion momentum spectroscopy. Both two-body and three-body fragmentation channels were observed with an ion-ion coincidence technique. The slopes of the islands in the coincidence spectrum were estimated and compared with other collision systems as well as theoretical predictions. Different results in fragmentation mechanisms were observed between our measurements and those from high incident electron energies [4]; it is attributed to the different states generated in different collision energies. Taking advantage of COLTRIMS, the momentum vectors of ionic fragments were measured and the momentum of the neutral particle was deduced; kinetic energy release distribution for the different fragmentation channels were thus obtained. The difference in KER distribution results confirmed the state difference explanation.

The three-body fragmentation in one- or two-step processes result in different signatures in the Dalitz plots. For the fragmentation channel $\text{C}^+ + \text{O}^+ + \text{O}$, it was found to be very similar to the 60 eV photon impact result: a significant contribution from the two-step channel $\text{CO}_2^{2+} \rightarrow \text{CO}^+ + \text{O}^+ \rightarrow \text{C}^+ + \text{O}^+ + \text{O}$ was distinguished. Contributions from the concerted process and deferred charge separation were also identified and discussed.

ACKNOWLEDGMENTS

This work was supported by the National Magnetic Confinement Fusion Program under Grant No. 2009GB106001, IAEA (CRP; No. 15735), and the National Science Foundation of China under Contract No. 11404065. This work was also supported by the Shanghai Leading Academic Discipline Project (Project No. B107).

- [1] J. Laksman, E. P. Månsson, C. Grunewald, A. Sankari, M. Gisselbrecht, D. Céolin, and S. L. Sorensen, *J. Chem. Phys.* **136**, 104303 (2012).
- [2] J. Li, Z. Zhao, J. Ye, and X. Zhang, *Phys. Rev. A* **86**, 052703 (2012).
- [3] C. Wu, C. Wu, D. Song, H. Su, Y. Yang, Z. Wu, X. Liu, H. Liu, M. Li, Y. Deng, Y. Liu, L.-Y. Peng, H. Jiang, and Q. Gong, *Phys. Rev. Lett.* **110**, 103601 (2013).
- [4] P. Bhatt, R. Singh, N. Yadav, and R. Shanker, *Phys. Rev. A* **85**, 042707 (2012).
- [5] M. R. Jana, P. N. Ghosh, B. Bapat, R. K. Kushawaha, K. Saha, I. A. Prajapati, and C. P. Safvan, *Phys. Rev. A* **84**, 062715 (2011).
- [6] J. H. D. Eland, L. Andric, P. Linusson, L. Hedin, S. Plogmaker, J. Palaudoux, F. Penent, P. Lablanquie, and R. Feifel, *J. Chem. Phys.* **135**, 134309 (2011).
- [7] R. K. Kushawaha, S. S. Kumar, I. A. Prajapati, K. P. Subramanian, and B. Bapat, *J. Phys. B: At., Mol. Opt. Phys.* **42**, 105201 (2009).
- [8] T. Masuoka, E. Nakamura, and A. Hiraya, *J. Chem. Phys.* **104**, 6200 (1996).
- [9] R. K. Singh, G. S. Lodha, V. Sharma, I. A. Prajapati, K. P. Subramanian, and B. Bapat, *Phys. Rev. A* **74**, 022708 (2006).
- [10] N. Saito, Y. Muramatsu, H. Chiba, K. Ueda, K. Kubozuka, I. Koyano, K. Okada, O. Jagutzki, A. Czasch, T. Weber, M. Hattass, H. Schmidt-Böcking, R. Moshhammer, M. Lavolle, and U. Becker, *J. Electron Spectrosc. Relat. Phenom.* **141**, 183 (2004).
- [11] C. Dimopoulou, M. E. Galassi, R. Moshhammer, R. D. Rivarola, D. Fischer, C. Hhr, and J. Ullrich, *J. Phys. B: At., Mol. Opt. Phys.* **38**, 3173 (2005).
- [12] N. Neumann, D. Hant, L. P. H. Schmidt, J. Titze, T. Jahnke, A. Czasch, M. S. Schöffler, K. Kreidi, O. Jagutzki, H. Schmidt-Böcking, and R. Dörner, *Phys. Rev. Lett.* **104**, 103201 (2010).
- [13] J. H. Sanderson, T. Nishide, H. Shiromaru, Y. Achiba, and N. Kobayashi, *Phys. Rev. A* **59**, 4817 (1999).
- [14] P. Moretto-Capelle, D. Bordenave-Montesquieu, and A. Bordenave-Montesquieu, *J. Phys. B: At., Mol. Opt. Phys.* **33**, L539 (2000).
- [15] B. Siegmann, U. Werner, H. O. Lutz, and R. Mann, *J. Phys. B: At., Mol. Opt. Phys.* **35**, 3755 (2002).
- [16] M. A. Parkes, J. F. Lockyear, S. D. Price, D. Schroder, J. Roithova, and Z. Herman, *PhysChemChemPhys* **12**, 6233 (2010).
- [17] H. C. Straub, B. G. Lindsay, K. A. Smith, and R. F. Stebbings, *J. Chem. Phys.* **105**, 4015 (1996).
- [18] C. Tian and C. R. Vidal, *Phys. Rev. A* **58**, 3783 (1998).
- [19] B. Bapat and V. Sharma, *J. Phys. B: At., Mol. Opt. Phys.* **40**, 13 (2007).
- [20] S. J. King and S. D. Price, *Int. J. Mass Spectrom.* **272**, 154 (2008).
- [21] A. Lahmam-Bennani, E. M. S. Casagrande, and A. Naja, *J. Phys. B: At., Mol. Opt. Phys.* **42**, 235205 (2009).
- [22] L. J. Frasinski, P. A. Hatherly, K. Codling, M. Larsson, A. Persson, and C. G. Wahlstrom, *J. Phys. B: At., Mol. Opt. Phys.* **27**, L109 (1994).
- [23] G. R. Kumar, P. Gross, C. P. Safvan, F. A. Rajgara, and D. Mathur, *Phys. Rev. A* **53**, 3098 (1996).
- [24] A. Hishikawa, A. Iwamae, and K. Yamanouchi, *Phys. Rev. Lett.* **83**, 1127 (1999).
- [25] K. Zhao, G. Zhang, and W. T. Hill, *Phys. Rev. A* **68**, 063408 (2003).
- [26] J. P. Brichta, S. J. Walker, R. Helsten, and J. H. Sanderson, *J. Phys. B: At., Mol. Opt. Phys.* **40**, 117 (2007).
- [27] D. Pavičić, K. F. Lee, D. M. Rayner, P. B. Corkum, and D. M. Villeneuve, *Phys. Rev. Lett.* **98**, 243001 (2007).
- [28] S. Minemoto, T. Kanai, and H. Sakai, *Phys. Rev. A* **77**, 041401 (2008).
- [29] G.-Y. Chen, Z. W. Wang, and W. T. Hill, *Phys. Rev. A* **79**, 011401 (2009).
- [30] I. Bocharova, R. Karimi, E. F. Penka, J.-P. Brichta, P. Lassonde, X. Fu, J.-C. Kieffer, A. D. Bandrauk, I. Litvinyuk, J. Sanderson, and F. Légaré, *Phys. Rev. Lett.* **107**, 063201 (2011).
- [31] P. Bhatt, R. Singh, N. Yadav, and R. Shanker, *Phys. Rev. A* **82**, 044702 (2010).
- [32] R. Flammini, M. Satta, E. Fainelli, G. Alberti, F. Maracci, and L. Avaldi, *New J. Phys.* **11**, 083006 (2009).
- [33] V. Sharma, B. Bapat, J. Mondal, M. Hochlaf, K. Giri, and N. Sathyamurthy, *J. Phys. Chem. A* **111**, 10205 (2007).
- [34] B. Wei, Z. Chen, X. Wang, D. Lu, S. Lin, R. Hutton, and Y. Zou, *J. Phys. B: At., Mol. Opt. Phys.* **46**, 215205 (2013).
- [35] Y. Zhang, X. Wang, D. Lu, B. Wei, B. Zhang, Y. Tang, R. Hutton, and Y. Zou, *Nucl. Instrum. Methods Phys. Res., Sect. B* **337**, 39 (2014).
- [36] S. Lin, Z. Chen, B. Wei, X. Wang, D. Lu, R. Hutton, and Y. Zou, *Phys. Scr.* **T144**, 014059 (2011).
- [37] X. Wang, K. Schneider, A. Kelkar, M. Schulz, B. Najjari, A. Voitkiv, M. Gundmundsson, M. Grieser, C. Krantz, M. Lestinsky, A. Wolf, S. Hagmann, R. Moshhammer, J. Ullrich, and D. Fischer, *Phys. Rev. A* **84**, 022707 (2011).
- [38] B. Wei, Y. Zhang, X. Wang, D. Lu, G. C. Lu, B. H. Zhang, Y. J. Tang, R. Hutton, and Y. Zou, *J. Chem. Phys.* **140**, 124303 (2014).